LASER VELOCIMETER MEASUREMENTS IN THE LEAKAGE ANNULUS
OF A WHIRLING SHROUDED CENTRIFUGAL PUMP

J. M. Sivo, A. J. Acosta, C. E. Brennen, and T. K. Caughey
Division of Engineering and Applied Science
California Institute of Technology
Pasadena, California

T. V. Ferguson and G. A. Lee
Rocketdyne Division
Rockwell International Corporation
Canoga Park, California

ABSTRACT

Previous experiments conducted in the Rotor Force Test Facility at the California Institute of Technology have thoroughly examined the effect of leakage flows on the rotordynamic forces on a centrifugal pump impeller undergoing a prescribed circular whirl. These leakage flows have been shown to contribute substantially to the total fluid induced forces acting on a pump. However, to date nothing is known of the flow field in the leakage annulus of shrouded centrifugal pumps. No attempt has been made to qualitatively or quantitatively examine the velocity field in the leakage annulus. Hence the test objective of this experiment is to aquire fluid velocity data for a geometry representative of the leakage annulus of a shrouded centrifugal pump while the rotor is whirling using laser velocimetry. Tests are performed over a range of whirl ratios and a flowrate typical of Space Shuttle Turbopump designs. In addition to a qualitative study of the flow field, the velocity data can be used to anchor flow models.

NOMENCLATURE

d	Location across leakage gap measured normal from impeller shroud
H	Clearance between impeller shroud and housing
Q	Volumetric leakage flow rate
ε	Eccentricity of impeller's circular whirl orbit
ω	Main shaft radian frequency
Ω	Whirl radian frequency

INTRODUCTION

Previous experimental and analytical results have shown that discharge-to-suction leakage flows in the annulus of a shrouded centrifugal pump contribute substantially to the fluid induced rotordynamic forces (Adkins, 1988). Experiments conducted in the Rotor Force Test Facility (RFTF) at Caltech on an impeller undergoing a prescribed whirl have indicated that the leakage flow contribution to the normal and tangential forces can be as much as 70% and 30% of the total, respectively (Jery, 1986). Recent experiments at Caltech have examined the rotordynamic consequences of leakage flows and have shown that the rotordynamic forces are functions not only of the whirl ratio but also of the leakage flow rate and the impeller shroud to pump housing clearance. The forces were found to be inversely proportional to the clearance and a region of forward subsynchronous whirl was found for which the average tangential force was destabilizing. This region decreased with flow coefficient (Guinzburg, 1992a). In recent experimental work, the present Caltech authors demonstrated that when the swirl velocity within the leakage path is reduced by the introduction of ribs or swirl brakes on the housing, then a substantial decrease in both the destabilizing normal and tangential forces could be achieved (Sivo, 1993).The motivation for the present research is that no previous experiments have examined the flow field within the leakage annulus. No measurements have been made of the destabilizing swirl or tangential velocity or demonstrated the complex nature of the flow. Analytical models of such flows use bulk average velocities to examine the rotordynamic forces. Such bulk flow models may be seriously flawed

when it comes to estimating the meridional and tangential velocities. It is hoped that this present research will serve as preliminary insight into the complex nature of leakage flows.

TEST APPARATUS

The present experiments were conducted in the Rotor Force Test Facility (RFTF) at Caltech and were sponsored by Rocketdyne. The leakage flow test section of the facility is shown in Figure (1).

The working fluid is water. The main components of the test section apparatus consist of a solid or dummy impeller (or rotating shroud) made of acrylic, a housing (or stationary shroud) instrumented for pressure measurements, a rotating dynamometer (or internal force balance), an eccentric whirl mechanism (not shown) and a leakage exit seal ring. The solid acrylic impeller is used so that backscatter to the velocimeter is minimized. The surface of the stationary housing has been modified to accommodate an optical flat glass window to view the fluid in the annulus. The leakage flow annulus between the impeller and housing is inclined at 45° to the axis of rotation. The nominal clearance between the solid impeller and the housing can be varied by axial adjustment of the housing. The flow through the leakage path is generated by an auxiliary pump. The solid impeller is mounted on a spindel attached to the rotating dynamometer connected to a data acquisition system which permits measurements of the rotordynamic force matrix. Jery, 1986 and Franz, 1989 describe the operation of the dynamometer. The eccentric drive mechanism imposes a circular whirl orbit on the basic main shaft rotation. The radius of the circular whirl orbit (or eccentricity) can be varied. The seal ring at the leakage exit models a wear ring. The clearance between the seal ring and impeller face is adjustable. The test approach makes use of the Rocketdyne Laser 2-focus Velocimeter to aquire fluid velocities across the shroud cavity. A pseudo-time history is obtained by using the velocimeter's multi-windowing synchronizer capability. This time history allows correlation of the velocity data to the rotor whirl.

A Polytec model 4000 laser-2-focus (L2F) velocimeter was used to conduct the testing. This two-spot or transit type velocimeter employed a 1 watt argon ion laser in an optical head with a 450 mm focal length lens. During testing the laser was operated at a lower power level resulting in about 125 mW in each spot. The L2F acquired data in a coaxial backscatter mode which was a requirement given the physical constraints of the tester hardware. The electronic signal processing sub-section of the velocimeter included an
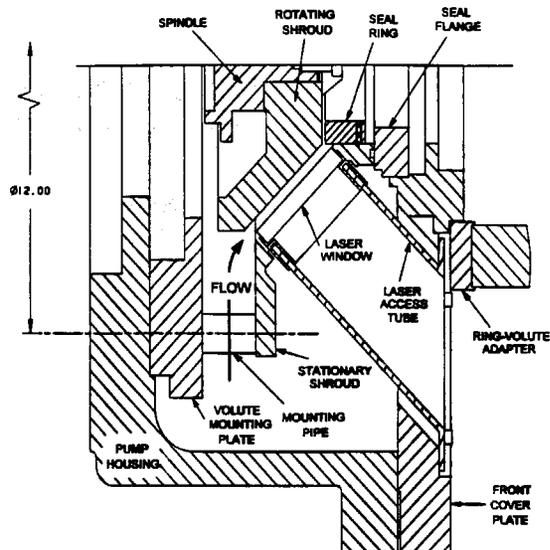

FIGURE 1. LEAKAGE FLOW TEST SECTION

analog time-to-pulse-height converter with a multichannel analyzer for display and accumulation of the data. Final reduction of the data was performed on a PC utilizing data reduction software from Polytec. Velocity and flow angles calculated from the time-of-flight and angular distributions, respectively, were output.

The L2F velocimeter in conjunction with an electronic synchronizer tagged the velocity and flow angle data relative to the whirl frequency of the impeller. Phase lock signals from the motor drive electronics were input to a strobe light. The rotating tester was viewed under the strobe light to determine the orbital position of the rotor when the whirl signal was generated. Sixteen circumferential zones or windows were generated by the synchronizer. Each window represents 22.5 degrees of rotation of the rotor during its whirl period. Therefore each window represents a pseudo-time history of the annulus flow as the orbital eccentricity of the impeller alternately squeezes and restores the nominal dimensions of the flow passage. The velocity and flow angle in each of these 16 windows was determined by the L2F.

The velocimeter was setup so the beams from the optical head were normal to the optical access window and concurrently to the surface of the impeller. Measurements were made in the plane normal to the propagation of the beam. The stop spot rotated about the start spot in this plane in order to explore for the direction of the flow vector.

The axial length of the measurement volumes was determined by the steep intensity gradient along the

beam axis. The measurement volume length can be defined as the space bounded by the points where the intensity in the beam was one-fourth of the maximum intensity at the waist, or in other words, where the beam radius has doubled. Using this definition, the length of the measurement volume was calculated to be 0.76 mm (0.030 inch).

The data were acquired through a rectangular-shaped window approximately 2.5 inches in length, 0.5 inches in height and 0.5 inches thick. The optical head (and hence the measurement volumes) was aligned with the test hardware by monitoring the speckle pattern reflected from the metal boundaries in the test hardware and the window frame. The accuracy of the speckle alignment data was validated by measurements made with depth micrometers. In addition, measurements were performed to assure the optical head was oriented normal to the optical access window so that the data collected across the annulus was in the same plane. Other measurements assured the head tracked level along the length of the window and that the relative angle between the zero angle position of the spots and the test hardware was quantified.

To improve the signal-to-noise ratio of the velocimeter measurements, the fluid was supplementally seeded with silver coated hollow glass micro-spheres. The mean particle size was 14 microns and the particle density was 1.4 gm/cm^3. A small quantity of the dry powdered spheres were mixed with distilled water. About 40-100 cc of this slurry was injected with a syringe into a pressure port located downstream of the test article. The particles, typically injected just before data collection at each measurement station, would circulate for about one hour in the closed loop test rig before settling out.

The L2F excels at measuring flows characterized by high velocity and low turbulence particularly in turbomachinery. Its performance efficiency in low velocity, high turbulence flows exemplified by this testing was not as good. A sufficient quantity of data was required for good statistical analysis of the time- of-flight and angular distributions in each of the 16 windows. Consequently, long run times were necessary. The information in Table 1 illustrates some of the parameters of the test. Overall, the number of data samples in each of the 16 windows was sufficient to yield an accuracy of at least $+/-2\%$ in velocity and generally closer to $+/-1\%$. The flow angle data is accurate to about $+/-1$ degree.

TEST MATRIX

This experiment is designed to measure the velocity of simulated leakage flows for different parameters such as whirl frequency ratio, axial location, and leakage annulus depth. For all tests a nominal annulus clearance H of 0.1072 in, a whirl eccentricity ε of 0.01in and a leakage exit face seal clearance of 0.02 in were maintained. Tests were conducted at a shaft speed ω of 2000 RPM and a leakage flow rate Q of 10 GPM. The above flow approximates the range of typical leakage rates for the new Space Shuttle Alternate Turbopump (ATP) presently being developed. Whirl ratios Ω/ω of 0.2, 0.3, 0.4 were tested. Velocity measurements were made at three meridional locations along the leakage path: Near Inlet (.6054 in), Near Midpoint (1.4054 in), Near Discharge (2.4054 in). The leakage path length along the impeller is 2.74 in. At each of these three stations, measurements were made at 5 depth locations across the leakage gap. Measuring from the solid impeller these positions were 0.0178 in (16.7%), 0.0357 in (33.4%), 0.0536 in (50%), 0.0715 in (66.7%), and 0.0893 in (83.3%).

The above test matrix is summarized in Table 2.

Table 1. Parameters of the Tests

whirl ratio	approximate average number of angles in a scan	average number of samples per angle	average data collection time (sec)	number of whirls over which data was averaged
0.2	35	51.667	.3581	23,885
0.3	42	50.000	.3880	38,800
0.4	36	51.545	.3851	51,346

Table 2. Velocimeter Measurements

RPM	Q (GPM)	Ω/ω	d (in)
2000	10	0.2	0.0178 (16.7%)
			0.0357 (33.4%)
			0.0536 (50.0%)
			0.0715 (66.7%)
			0.0893 (83.3%)
		0.3	0.0178 (16.7%)
			0.0357 (33.4%)
			0.0536 (50.0%)
			0.0715 (66.7%)
			0.0893 (83.3%)
		0.4	0.0178 (16.7%)
			0.0357 (33.4%)
			0.0536 (50.0%)
			0.0715 (66.7%)
			0.0893 (83.3%)

RESULTS FOR MEASUREMENTS OF MERIDIONAL VELOCITY

In the following results not all gap locations are reported. This is due to the low signal to noise ratio for gap locations near the impeller shroud surface.

Figure (2) shows plots of the absolute meridional velocity at a whirl ratio of 0.2 for the three meridional locations respectively. Looking at the Near Inlet figure it can be seen that reverse flow occurs for the 33.4% gap point between the whirl orbit angles of 110° and 260°. Further away from the impeller across the gap there is no reverse flow. Looking at the Near Mid-point figure reverse flow occurs again for the 33.4% gap point, but only for a smaller range of whirl orbit angles of 120° to 220°. Once again further away from the impeller across the gap there is no reverse flow. Looking at the Near Discharge figure, there is no evidence of reverse flow. Hence from the above it appears that there is recirculation near the surface of the impeller between the inlet to the leakage path and the midpoint.

Figure (3) shows similar plots except for a whirl ratio of 0.3. The Near Inlet figure shows that the 16.7% and 33.4% gap points are in reverse flow at all whirl orbit locations. For the Near Mid-point figure there is reverse flow between 120° and 200°. From the Near Discharge figure there is no evidence of reverse flow. Hence, once again it appears that there is a recirculation zone near the surface of the impeller between the inlet to the leakage path and the midpoint.

Figure (4) shows similiar plots except for a whirl ratio of 0.4. There is no evidence of recirculation, except in the Near Mid-point figure where there is recirculation for the 33.4% gap point at 150°.

As a general observation of all the above plots it can be seen that the meridional velocity is largest furthest from the rotating impeller and is quite large at the 83.3% gap point, which is closest to the stationary casing.

RESULTS FOR MEASUREMENTS OF TANGENTIAL VELOCITY

Figures (5) through (7) show the absolute tangential velocity for the three whirl ratios tested and five gap locations. A few general observations can be made. Near Inlet plots show the velocity profiles spread out with the largest tangential velocity nearest the impeller, as expected. Also except for the 0.4 whirl case, near discharge velocity profiles bunch up close to the impeller. It is as if a bulk tangential velocity is set up.

CONCLUSIONS

Laser velocimeter measurements have been made in the leakage annulus of a whirling shrouded impeller. Results clearly show regions of recirculation which diminish at higher whirl ratios. These recirculation regions are dominant near the entrance to the leakage path. In some cases these recirculation regions exist entirely around the impeller.

ACKNOWLEDGEMENTS

REFERENCES

Adkins, D. R. and Brennen, C. E., 1988, Analysis of Hydrodynamic Radial Forces on Centrifugal Pump Impellers, ASME J. Fluids Eng., Vol. 110, No. 1, pp. 20-28.

Franz, R. J., 1989, Experimental Investigation of the Effect of Cavitation on the Rotordynamic Forces on a Whirling Centrifugal Pump Impeller, Ph.D. Thesis, California Institute of Technology.

Guinzburg, A., 1992a, Rotordynamic Forces Generated By Discharge-To-Suction Leakage Flows in Centrifugal Pumps, Ph.D. Thesis, California Institute of Technology.

Jery, B., 1986, Experimental Study of Unsteady Hydrodynamic Force Matrices on Whirling Centrifugal Pump Impellers, Ph.D. Thesis, California Institute of Technology.

Sivo, J. M., Acosta, A. J., Brennen, C. E. and Caughey, T. K., 1993, The Influence of Swirl Brakes on the Rotordynamic Forces Generated by Discharge-To-Suction Leakage Flows in Centrifugal Pumps, presented at the ASME Second Pumping Machinery Symposium, Washington, D. C., June 20-24, 1993.

Zhuang, F., 1989, Experimental Investigation of the Hydrodynamic Forces on the Shroud of a Centrifugal Pump Impeller, E249.9, Division of Engineering and Applied Science, California Institute of Technology.
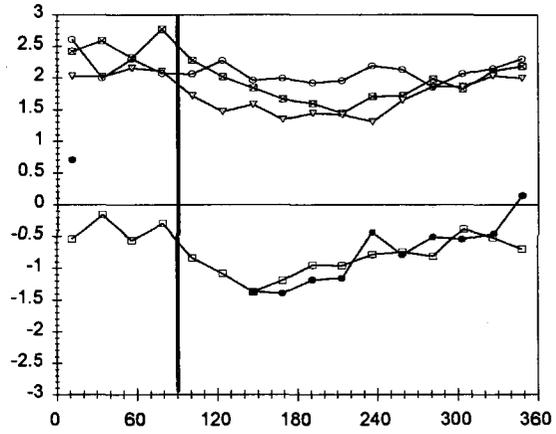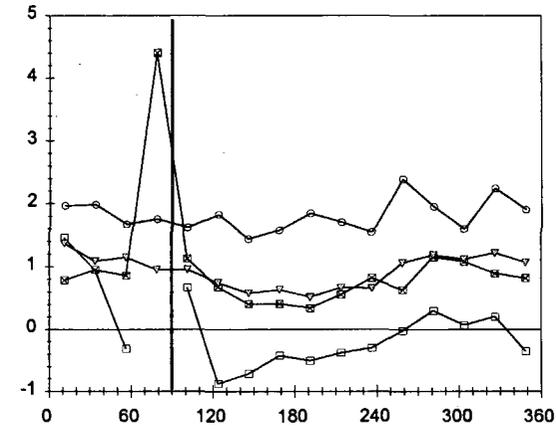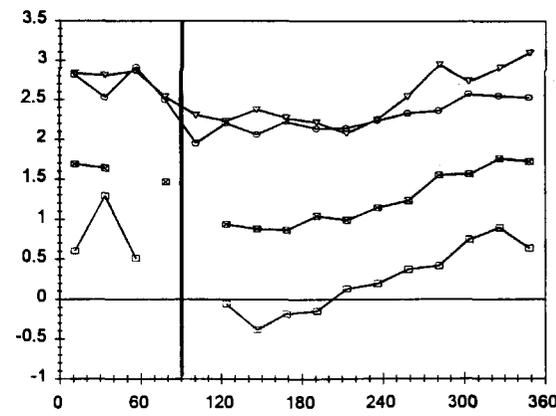
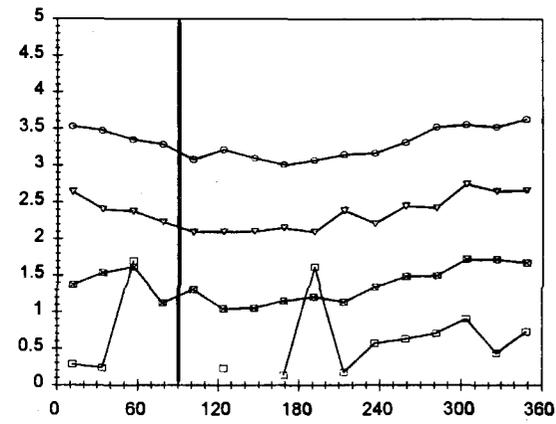# Meridional Velocity

$\Omega/\omega = +0.2$

$\Omega/\omega = +0.3$
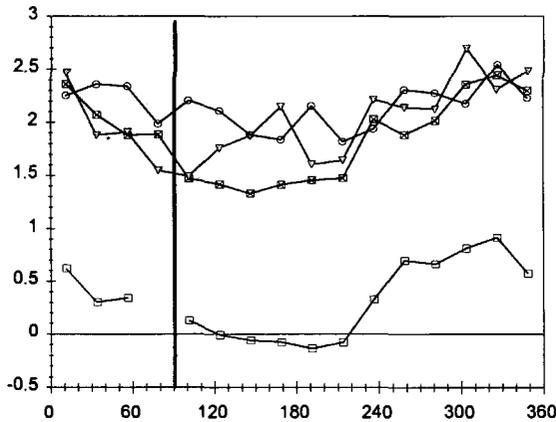
Near Inlet
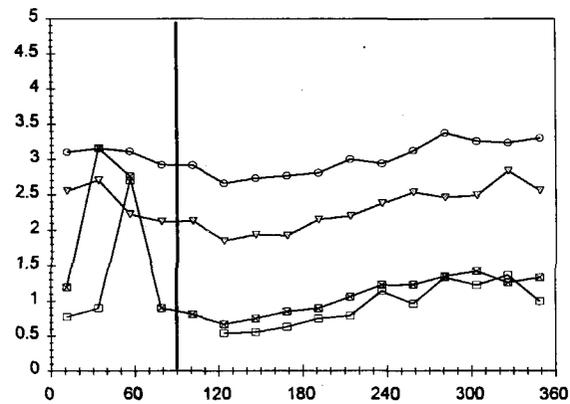
Mid-Point

Near Discharge

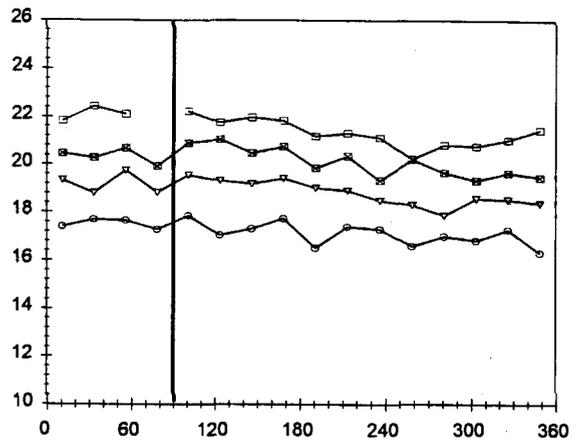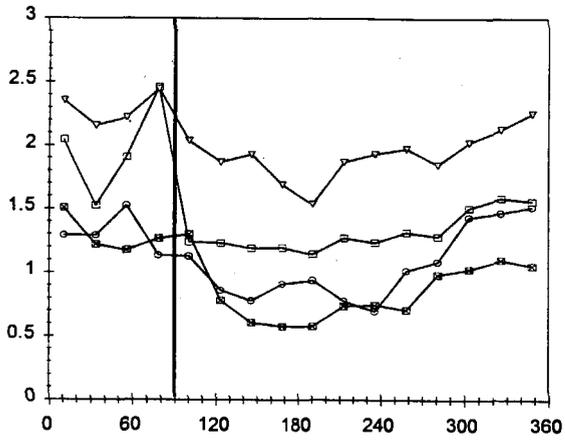**Location in Whirl Orbit (deg)**

FIGURE 2.

115

FIGURE 3.

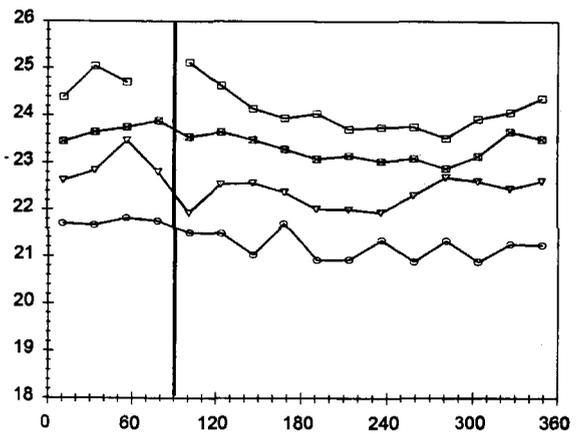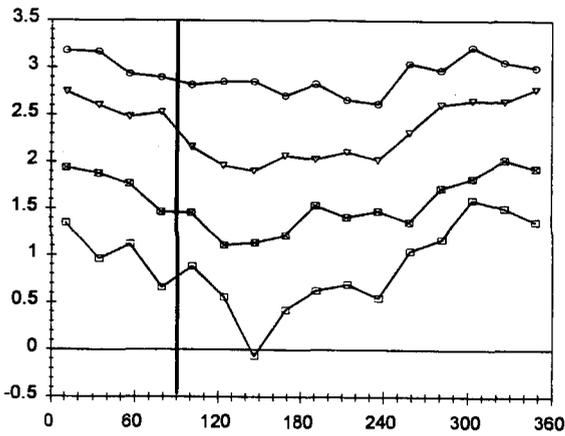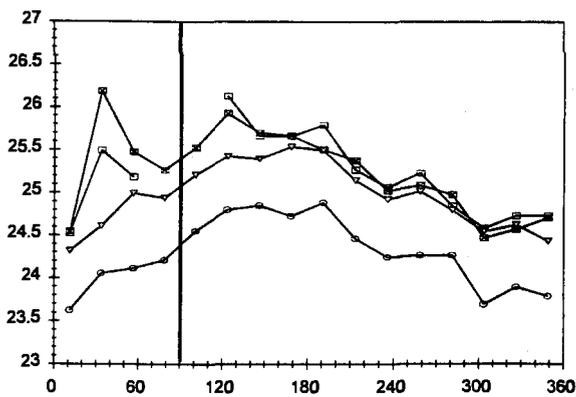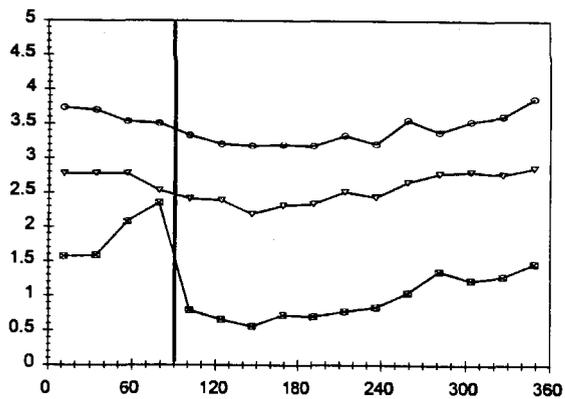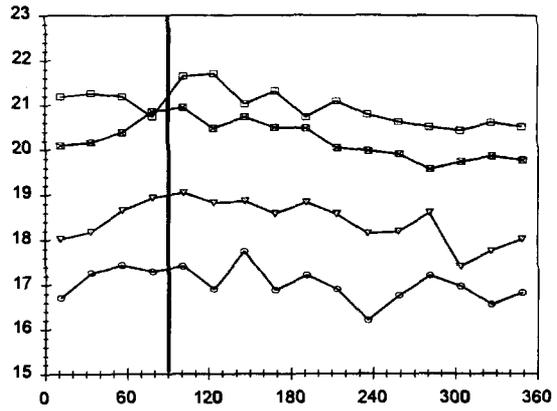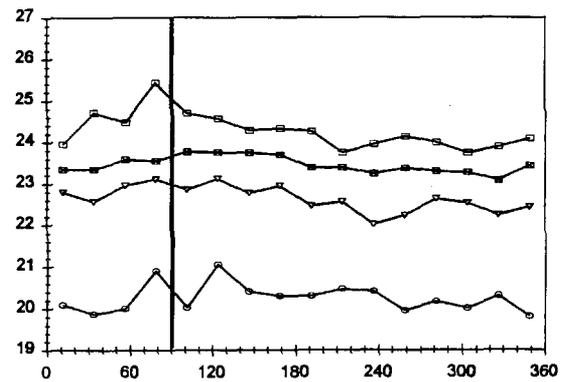**Meridional Velocity**   **Tangential Velocity**

$\Omega/\omega = +0.4$ $\Omega/\omega = +0.2$

Near Inlet

Mid-Point

Near Discharge

Location in Whirl Orbit (deg)

FIGURE 4.   116   FIGURE 5.
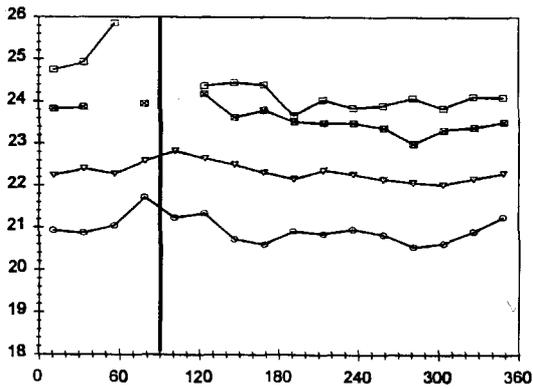
Tangential Velocity

$\Omega/\omega = +0.3$

$\Omega/\omega = +0.4$

Near Inlet

Mid-Point

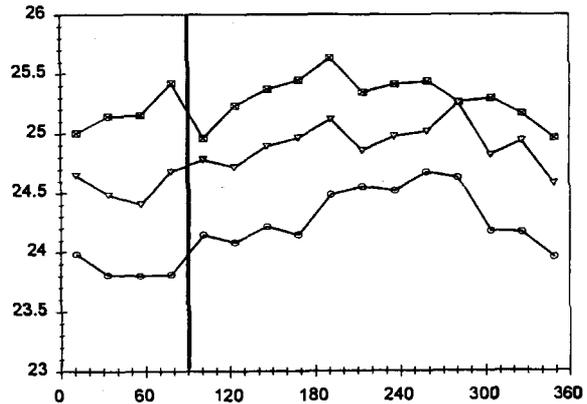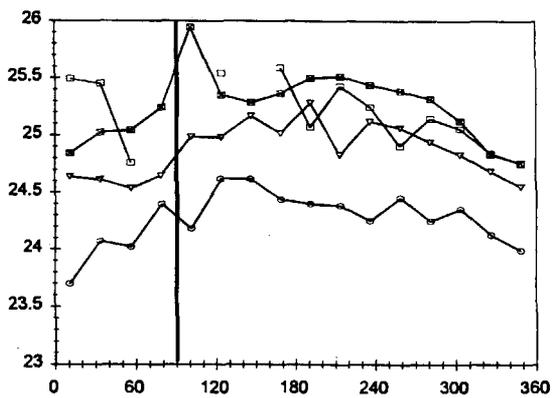**Near Discharge**

Location in Whirl Orbit (deg)

FIGURE 6.   117   FIGURE 7.